arXiv:1302.2265v1 [nucl-ex] 9 Feb 2013

Proton-induced fission of heavy nuclei at intermediate energies

A. Deppman[*]
Instituto de Fisica, Universidade de São Paulo, P. O. Box 66318, 05315-970 São Paulo, SP, Brazil

E. Andrade-II[†]
Instituto de Fisica, Universidade de São Paulo, Rua do Matao,
Travessa R 187, 05508-900 São Paulo, SP, Brazil

V. Guimarães[‡] and G. S. Karapetyan[§]
Instituto de Fisica, Universidade de São Paulo, P. O. Box 66318, 05389-970 São Paulo, SP, Brazil

A. R. Balabekyan[¶]
Yerevan State University, Alex Manoogian 1, Yerevan 0025, Armenia

N. A. Demekhina[**]
Yerevan Physics Institute, Alikhanyan Brothers 2, Yerevan 0036, Armenia
Joint Institute for Nuclear Research (JINR), Flerov Laboratory of Nuclear Reactions (LNR),
Joliot-Curie 6, Dubna 141980, Moscow region Russia

The intermediate energy proton-induced fission of ^{241}Am, ^{238}U and ^{237}Np is studied. The inelastic interactions of protons and heavy nuclei are described by a CRISP model, in which the reaction proceeds in two steps. The first one corresponds fast cascade, where a series of individual particle-particle collisions occurs within the nucleus. It leaves a highly excited cascade residual nucleus, assumed to be in thermal equilibrium. Subsequently, in the second step the excited nucleus releases its energy by evaporation of neutrons and light charged particles as well. Both the symmetric and asymmetric fission are regarded, and the fission probabilities are obtained from CRISP code calculations, by means of statistical weighting factors. The fission cross sections, the fissility of the fissioning nuclei, and the number of nucleons lost by the target – before and after fission – are calculated and compared to experiments for 660 MeV protons incident on ^{241}Am, ^{238}U and ^{237}Np. Some of the model predictions are in full compliance to the experiments. We conclude that our two step model provides a reasonable description of the medium energy proton-induced fission.

PACS numbers: 25.85.Ge

I. INTRODUCTION

The interaction between high energy protons and atomic nuclei has been studied over the last fifty years. Such a continuous interest in this subject is caused by many reasons. First of all, proton-induced nuclear reactions are very interesting, since they involve both fundamental problems, i.e. nucleon - nucleon interaction and properties of the nuclei in various conditions of excitation. Furthermore, modification of the proton energy and/or target nucleus leads to a rich spectrum of phenomena, which have to be understood and described theoretically.

The understanding of the mechanism of proton-nucleus collisions is prerequisite for understanding of much more complicated mechanism concerning heavy ions collisions. It is expected that the proton collisions with atomic nuclei do not cause significant compression or deformation of nuclei. Therefore, the description of proton-induced reactions should be less complex than reactions induced by heavy-ion collisions.

The study of proton-nucleus collisions is a source of experimental data which are extremely important for scientific and technological applications. These data must cover practically full list of the atomic nuclei studied in a broad range of proton energies from MeV to tens of GeV. It is, of course, almost impossible to measure all necessary data.

---

[*] Electronic address: deppman@if.usp.br
[†] Electronic address: esegundo@if.usp.br
[‡] Electronic address: valdirg@dfn.if.usp.br
[§] Electronic address: ayvgay@ysu.am
[¶] Electronic address: balabekyan@ysu.am
[**] Electronic address: demekhina@nrmail.jinr.ru

Thus one must rely on the theoretical models or parameterizations, which are able to interpolate and extrapolate the experimental information to the targets or energies not available experimentally yet.

In order to validate and to test theoretical models for various ranges of target mass and proton beam energy, the set of reliable data consisting of inclusive and exclusive observables should be available. The present situation, both experimentally as well as theoretically is rather puzzling. In spite of long history of investigations of proton-nucleus reactions neither the predictive power of available theoretical models reached demanded accuracy, nor the experimental data basis is rich enough to serve as the benchmarks, which may put very restrictive demands and constraints to the theoretical description. The theoretical models are not able to reproduce the full amount of the observed phenomena and frequently they allow only for ambiguous interpretation of the observed facts.

The present work is devoted to the discussion of the CRISP model calculations for the description of multimodal fission for proton-heavy target (^{241}Am, ^{238}U, ^{237}Np) collisions at 600 MeV energy of incident particles. The experiments considered are described in detail elsewhere [1, 2].

II. THE CRISP CODE

CRISP is a Monte Carlo code for simulating nuclear reactions [3] that uses a two step process. First, an intranuclear cascade is simulated, following a time-ordered sequence of collisions in a many-body system [4, 5]. Besides, when the intranuclear cascade finishes, the evaporation of nucleons and alpha-particles starts to compete with fission [6].

In the simulation, the reactions can be initiated by intermediate and high energy protons [5] or photons [7–9]. It has been extended to energies up to 3.5 GeV [10], and it was shown that the CRISP code can provide good results for the total photonuclear absorption cross sections from approximately 50 MeV, where the quasi-deuteron absorption mechanism is dominant, up to 3.5 GeV, where the so-called photon-hadronization mechanism is dominant. It leads to a shadowing effect in the cross section [10]. One important feature in the simulation of the intranuclear cascade is the Pauli blocking mechanism, which avoids violation of the Pauli principle. In CRISP, a strict verification of this principle is performed at each step of the cascade, resulting in a more realistic simulation of the process. The advantages of such an approach have been further discussed elsewhere (see [3] and references therein).

In the evaporation/fission competition that follows intranuclear cascade, Weisskopf's model is adopted for calculating the branching ratios of the evaporating channels, which includes evaporation of neutrons, protons, and alpha-particles [6, 8, 9]. The Bohr-Wheeler model is adopted for the fission process. The code has provided photofission cross sections in full compliance to experimental data [3]. The CRISP code has already been used for evaluating mass distributions of fragments for fission induced by photons at intermediate energies [11], and to calculate spallation yields and neutron multiplicities for reactions induced by high energy protons [12], giving results in good agreement with experimental data. In addition, the code has already been used in studies of the ADS (Accelerator Driving System) nuclear-reactors [12–15].

III. DESCRIPTION OF MODEL AND CALCULATION

Theoretically, the fission process has been successfully described by the Multimodal - Random Neck Rupture Model (MM-NRM) [16–18], which takes into account the collective effects of nuclear deformation during fission through a liquid-drop model. Furthermore, it includes single-particle effects through microscopic shell-model corrections. The microscopic corrections create valleys in the space of elongation and mass number, each valley corresponding to one different fission mode [18].

The yield of fragments, characterized by A (the fragment mass number) and Z (the atomic number), is determined for each mode by a Gaussian distribution. In the following we consider that the fission can take place through three modes: a symmetric mode and two asymmetric modes. The total yield is obtained by the sum of the three Gaussian functions, as [19]:

$$\begin{aligned} Y_A \;=\; \frac{1}{\sqrt{2\pi}}\Bigg[& \frac{K_{1AS}}{\sigma_{1AS}}\exp\left(-\frac{(A-\bar{A}_S-D_{1AS})^2}{2\sigma_{1AS}^2}\right)+\frac{K'_{1AS}}{\sigma'_{1AS}}\exp\left(-\frac{(A-\bar{A}_S+D_{1AS})^2}{2\sigma'^2_{1AS}}\right)+ \\ & \frac{K_{2AS}}{\sigma_{2AS}}\exp\left(-\frac{(A-\bar{A}_S-D_{2AS})^2}{2\sigma_{2AS}^2}\right)+\frac{K'_{2AS}}{\sigma'_{2AS}}\exp\left(-\frac{(A-\bar{A}_S+D_{2AS})^2}{2\sigma'^2_{2AS}}\right)+\frac{K_S}{\sigma_S}\exp\left(-\frac{(A-\bar{A}_S)^2}{2\sigma_S^2}\right)\Bigg], \end{aligned} \quad (1)$$

where $\bar{A}_S$ is the mean mass number determining the center of Gaussian functions; and K_i, σ_i, and D$_i$ are the contribution, dispersion and position parameters of the i^{th} Gaussian functions. The indexes AS, S designate the asymmetric and symmetric components.

The fragment charge distribution can be estimated by using the approximation with Gaussian functions in the form [20, 21]:

$$Y_{A,Z} = \frac{Y_A}{\Gamma_z \pi^{1/2}} \exp\left(-\frac{(Z-Z_p)^2}{\Gamma_z^2}\right), \tag{2}$$

where $Y_{A,Z}$ is the independent yield of the nuclide (Z, A). The values Y_A (the total chain yield for given mass number A), Z_p (the most probable charge for Z distribution isobars with mass number A) and Γ_z (the width parameter). The values Z_p and Γ_z can be represented as slowly varying linear functions of the mass numbers of fission fragments:

$$\begin{aligned} Z_p &= \mu_1 + \mu_2 A, & (3)\\ \Gamma_z &= \gamma_1 + \gamma_2 A, & (4) \end{aligned}$$

where μ_1, μ_2, γ_1 and γ_2 are adjustable parameters.

The yield, the position, and the width parameters for each mode in Eq. (1) and μ_1, μ_2, γ_1, and γ_2 in Eqs. (3) and (4) are usually considered free parameters for fitting procedure. This method has been used for describing spontaneous fission [22], low-energy induced fission [23–25], fission induced by thermal-neutrons [26–28] and 12 MeV protons [29], and even for fission induced by intermediate energy probes such as 190 MeV protons [21], neutrons at energies up to 200 MeV [30], and also by heavy-ions [31, 32].

Since the CRISP code simulates the entire process up to the point of fission, the fissioning nucleus of all events is known. Hence $\bar{A}_S$ is not taken as a free parameter, but as a distribution instead. Therefore, at every point of decision on the fission channel the appropriate value for $\bar{A}_S$ is used considering the nucleus which is undergoing fission.

Whenever the fission channel is chosen, the masses and atomic numbers of the heavy fragments produced, A_H and Z_H, respectively, are sorted according to equation (3). The light fragments are obtained according to $A_L = A_f - A_H$ and $Z_L = Z_f - Z_H$, where A_f and Z_f are the mass and atomic number of the fissioning nucleus, respectively.

As a final step, all fragments obtained in the above fashion evaporate according to the model of evaporation/fission competition already mentioned. The energy of each fragment is determined using

$$E_i = \frac{A_i}{A_f} E_{frag}, \tag{5}$$

where E_i and A_i are the excitation energy and the mass number of the fragment i, respectively. E_{frag} is the total excitation energy of the fragments, which is assumed to be equal to the excitation energy of the fissioning system.

IV. RESULTS AND DISCUSSION

The investigation of the fission processes under these extreme conditions is expected to provide relevant information on the dynamics of fission at high excitation energies. It is well known that the formation of fragments in the fission process, including its nucleon composition, occurs before the final division of the nucleus. The excitation energy of the nuclear system and fragments usually is removed by evaporation of nucleons, mostly neutrons and γ-quanta. The number of emitted neutrons from the compound nucleus (pre-scission neutrons), as well as from the fragments (post-scission neutrons), is a function of the projectile energy, the deformation of the fissioning nucleus, and the structural characteristics of the products.

The substantial part of the initial excitation energy leads to a wide distribution of final fragment states. Therefore, they are characterized by a large spectra of mass, charge and kinetic energy.

At high proton bombarding energy, as the energy excitation increases, the pre-scission neutrons multiplicity and contribution from different compound nuclei to the post-scission particle emission grow, the mass and energy distributions of fissioning nuclei and the fission products are raised significantly [33, 34].

Fragments that represent the final products of the fission process after neutrons and γ-rays emission from the fissioning nucleus and the primary fragments, are detected, in the off-line experiment. Measurements of the charge, mass, energy, and spin distributions of these products, as well as the systematization of the data within various model representations, can provide prominent information about the properties of primary fragments and the mechanism of their formation.

A. Charge Distribution

It is assumed that the charge distribution of the fission fragments is well described by a Gaussian function (2) and is characterized by parameters such as the most probable charge (Z_p) for the isobaric chains A and the width parameter (Γ_z). Experimental values of the most probable charge are removed from the line of β-stability on the several charge units. As the excitation energy and the atomic number of the fissioning nucleus increase, the number Z_p of isobaric chains becomes closer to the values Z for the stable nuclei. Another parameter, that determines the charge distribution of the fragments, is the dispersion of the distribution, or the width parameter (Γ_z). Usually one uses this parameter, averaged over the entire spectrum of the fragment mass numbers. As the excitation energy increases, the values for Γ_z rises and the charge distribution becomes broader. The parameters of the charge distribution determine the total isobaric yield of the mass, corresponding to different isobaric chains. The results of the analysis performed in [1, 2] revealed that Z_p and Γ_z can be represented as slowly varying linear functions of the mass numbers of fission fragments (3), (4).

The deviation of experimental widths from the values calculated for the targets ^{241}Am, ^{238}U, and ^{237}Np at proton energy 660 MeV is plotted in Figure 1 (a, b, c). The values for χ^2 are as follows: in the case of ^{241}Am is $\chi^2 = 0.022$, in the case of ^{238}U is $\chi^2 = 0.012$, in the case of ^{237}Np is $\chi^2 = 0.017$.

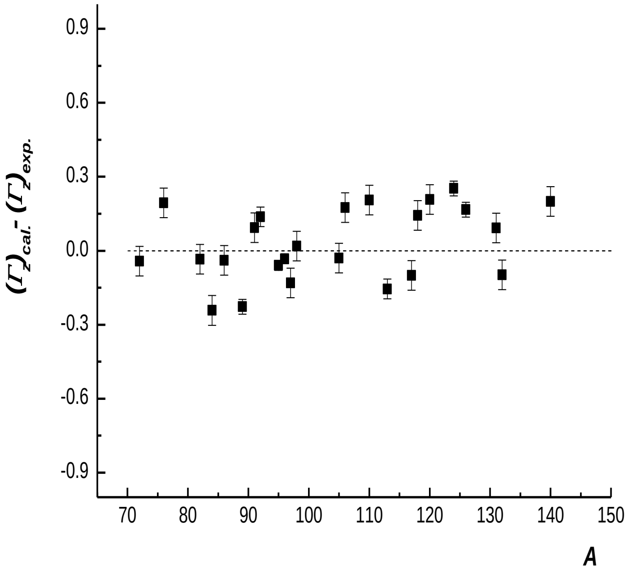

0.9
0.6
0.3
0.0
-0.3
-0.6
-0.9
$(\Gamma_z)_{cal.}-(\Gamma_z)_{exp.}$
70
80
90
100
110
120
130
140
150
A

a)

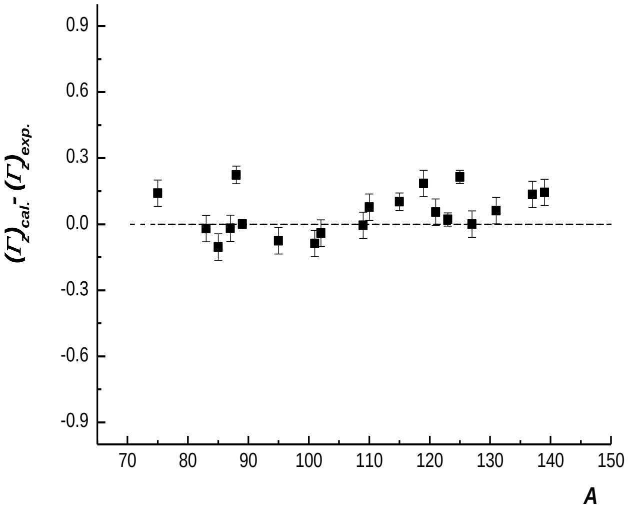

0.9
0.6
0.3
0.0
-0.3
-0.6
-0.9
$(\Gamma_z)_{cal.}-(\Gamma_z)_{exp.}$
70
80
90
100
110
120
130
140
150
A

b)

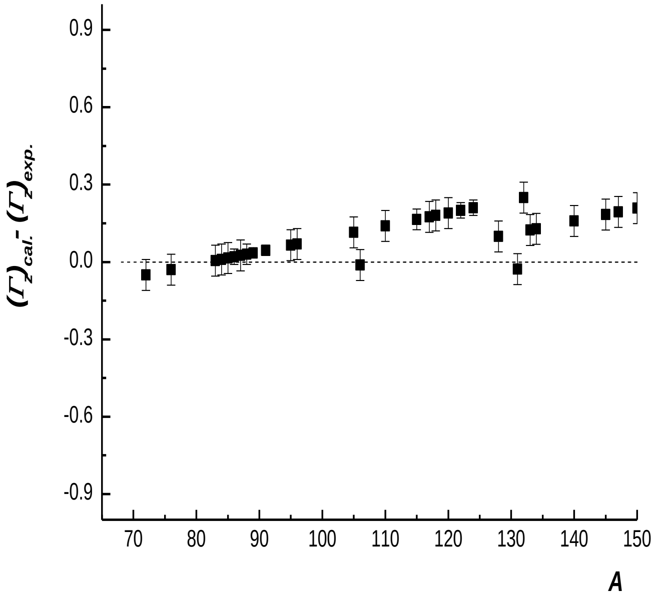

c)

FIG. 1: The deviation of experimental width of charge distribution from calculated by CRISP code for ^{241}Am (a), ^{238}U (b) and ^{237}Np (c) targets.

From the values of χ^2 it is shown that the code reproduces quite well the experimental widths of charge distribution. However, we can stress out several trends of above mentioned comparison. The deviation is larger for the ^{241}Am target. All ranges of mass number show almost the same behavior independent of the fission mode. It was found that best agreement with the experimental results was obtained for^{238}U. Small discrepancies in the range of asymmetric peaks can be caused by uncertainties in the measuring of the experimental cross-sections and lack of measured nuclide in the mass chain. For the ^{237}Np the model describe range of light asymmetric peak. Agreement becomes less for symmetric high-energy fission and heavy asymmetric peak, where the difference of the widths rises with mass number. But there is unexpected behavior between measured and predicted data. The dependence has a minimum at the mass values in the interval $A = 132 - 135$ connected with shells $Z = 50$ and $N = 82$ and neighborhood nuclides. Such result is inconsistent with the assumption that the shell effects vanish with increasing of excitation energy [34].

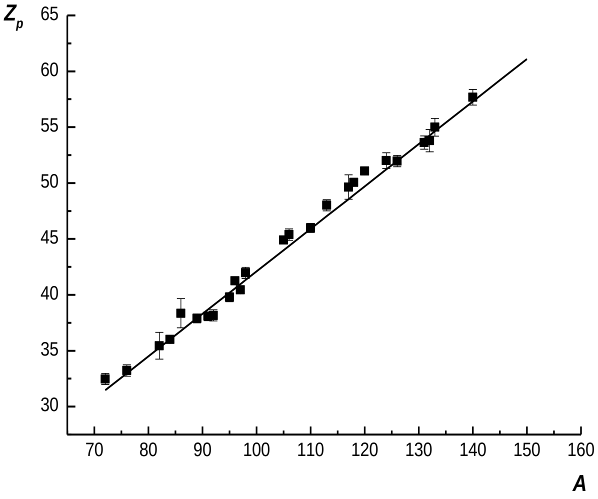

Z_p
65
60
55
50
45
40
35
30
70
80
90
100
110
120
130
140
150
160
A

a)

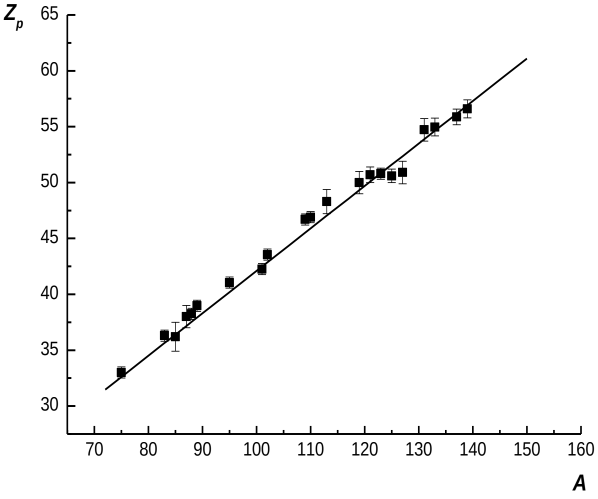

Z_p
65
60
55
50
45
40
35
30
70
80
90
100
110
120
130
140
150
160
A

b)

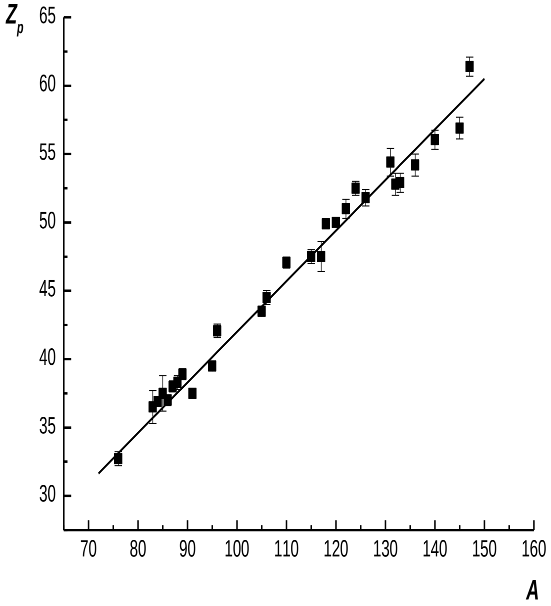

c)

FIG. 2: The most probable charge Z_p for ^{241}Am (a), ^{238}U (b) and ^{237}Np (c) targets, respectively: the calculations by CRISP (thick black solid line), experimental data (■).

Figure 2 shows both the experimental values of the most probable charge Z_p and the values, calculated by the CRISP model for ^{241}Am, ^{238}U and ^{237}Np. The calculated criterion χ^2 were: ^{241}Am–$\chi^2 = 0.57$, ^{238}U–$\chi^2 = 0.63$ ^{237}N–$\chi^2 = 1.05$.

As it can be seen from the Figure 2, for ^{241}Am and ^{238}U calculations reveals full complianc with experiments. Deviation is observed for ^{237}Np. The experimental charges mainly shifts to the proton-rich side relative to the model predictions almost for all fragment mass numbers.

In general, more precise agreement to with the calculation obtained for ^{238}U nucleus and less for ^{241}Am and ^{237}Np. This result can be understood in the frame of neutron evaporation process.

As it is known,the increase of excitation energy serves the purpose of opening new fission channels by means of particle evaporation prior to the actual scission of the excited nucleus [33]. In the case of interaction with intermediate- and high-energy particles, the fission process is considered at a slow reaction stage after the completion of the internuclear cascade and the formation of an excited after-cascade nucleus. Neutron evaporation is a process that competes with the fission process (proton emission is suppressed). These processes proceed sequentially in several steps, depending on the excitation energy. At each step, the residual nucleus may undergo fission or emit a neutron. As a result, there exists a set of various fissioning nuclides with different excitation energy. In the case of heavy actinides (Am, Np), more neutron evaporates and, as a consequence, we have wide distribution of fissioning nuclei because of the contribution of the neutron-deficient fission of nuclei formed after the emission of neutrons. There is difficult to take into account all aspects of such process in actual calculation process.

However, an analysis of parameter values shows that in general the CRISP model fairly well describes the charge distribution for proton-induced fission. It can be assumed that the model takes into account the main properties of fissile systems and provide a universal way to predict the characteristics of the fragment charge distribution.

B. Mass Distribution

The study of multi-modal nature of nuclear fission is an important and interesting area of current research in nuclear physics. Interest of this area is caused by the need to understand the nature of the formation fission fragment mass-energy distributions (MEDs). The multi-modal concept is based on the assumption that experimental MEDs are a superposition of MEDs of individual fission modes. These modes are caused by the valley structure of the deformation potential energy surface. The attempt to separate and quantitatively describe above mentioned processes makes it possible to understand the influence of the nuclear structures on the fission nature.

The application of the hypothesis of the multimodal fission allowed to extract the different components on the base of the decomposition of the mass yield curve. At present it is supposed that there are three distinct fission modes for the heavy nuclei – symmetric (Superlong) mode and two asymmetric modes – Standard I and Standard II [18]. Superlong mode fragments are strongly elongated with masses around $A_f/2$. Standard I mode is characterized by high kinetic energies of fission fragments. Heavy fragment is spherical with $M_H \sim 132$, $Z_H \sim 50$ and $N_H \sim 82$. Kinetic energies of Standard II mode fragments are lower than those of Standard I mode. Heavy fragment with $M_H \sim 140$ is slightly deformed, influenced by the deformed neutron shell closure$N_H \sim 88$ and $Z_H \sim 52$.

By using the calculated values of σ_A that correspond to the total fission cross-section of a fragment for a specific mass number (2) made it possible to construct the mass yield for three fissioning nuclei. Integrating over the Gaussian and multiplying with a factor 2, because of the two fission fragments in each fission event, gives an estimate for the total fission cross-section. The values for the total fission cross-sections σ_{tot} determined in this way together with calculated by CRISP code are given in Table 1. In Table 1 the following values are also given: the mean mass of the mass distribution ($\overline{A}_S$); mean mass of the fissioning nucleus ($(A_f)_{cal}$) after evaporation of pre-scission neutrons from compound nucleus; mean mass of the fissioning nucleus ($(A_{ff})_{cal}$) after evaporation of post-scission neutrons from fragments; experimental mean mass of the fissioning nucleus $(A_f)_{exp}$, which includes both type of evaporated neutrons. The total fission mass-yield distributions at $E_p = 660$ MeV is shown in Figure 3 (a, b, c) for ^{241}Am, ^{238}U and ^{237}Np, respectively, as a function of the product mass number (A).

Table 1. Parameters of the mass distributions.

Parameter	^{241}Am	^{238}U	^{237}Np
$(\sigma_{tot})_{exp}$, mb	1763.7±265.0	1226.0±183.9	1600.0±240.0
$(\sigma_{tot})_{cal}$, mb	1081.0	951.0.8	1069.0
$(\bar{A}_S)_{exp}$	113.5±0.6	113.5±0.6	111.7±0.9
$(\bar{A}_S)_{cal}$	113.0	114.0	111.5
$(A_f)_{exp}$	227.0	227.0	223.4
$(A_{ff})_{cal}$	226.0	228.0	223.0
$(A_f)_{cal}$	237.7	232.5	234.7

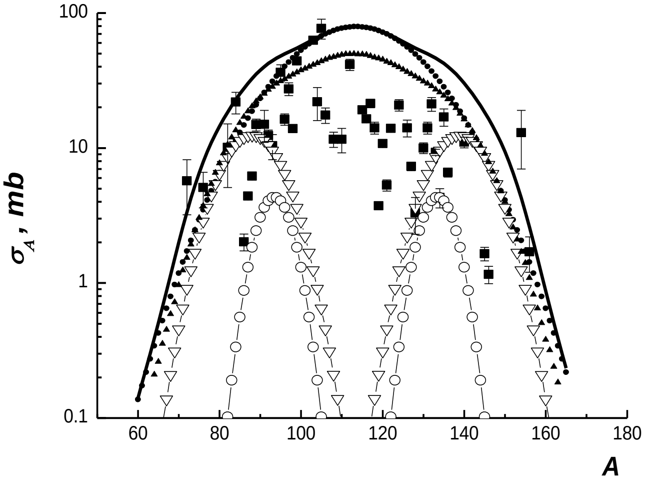
100
10
1
0.1
σ_A, mb
60
80
100
120
140
160
180
A

a)

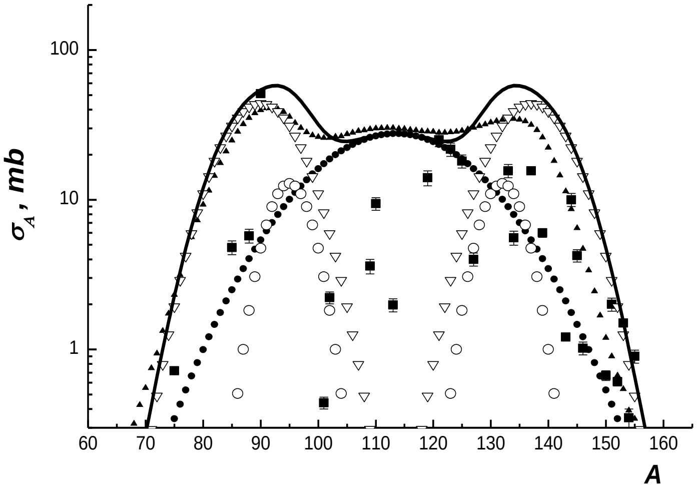
100
10
1
σ_A, mb
60
70
80
90
100
110
120
130
140
150
160
A

b)

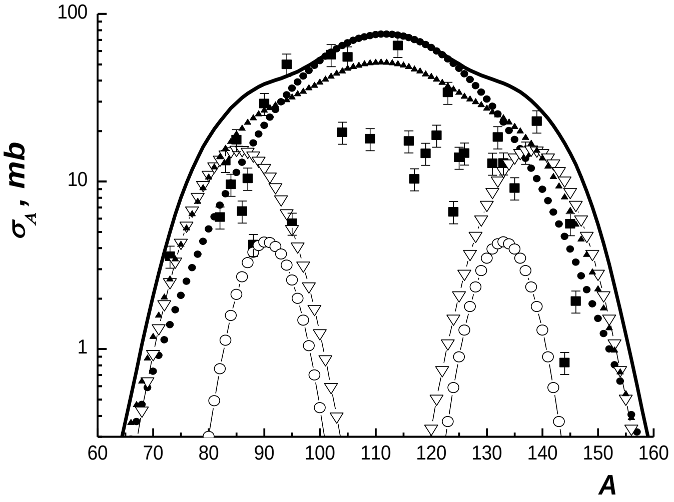

c)

FIG. 3: Components of mass yield at $E_p = 660$ MeV for ^{241}Am (a), ^{238}U (b) and ^{237}Np (c) targets: Superlong mode(●), Standard I mode (○), Standard II (△), total experimental cross-section ($\sigma_{tot\,exp}$) (thick line), total calculated yield $(\sigma_{tot})_{cal}$ (▲), experimental points (■).

The results by CRISP code calculations allowed to provide an overview on the distributions for ^{241}Am, ^{238}U and ^{237}Np. The agreement between the calculation and the experimental data is fairly good. The code reproduces totally the shape of the distribution (position of the mean mass as well as mean mass of the fissioning nucleus after evaporation of post-scission neutrons). This fact shows that the model correctly takes into account the contribution of the symmetric and asymmetric modes. However, it should be mentioned that the code underestimates the absolute values of total fission cross-section σ_{tot}. Especially, the deviation from experimental data is large for heavier actinides (Am, Np). And as it was mentioned in previous section, for such actinides there is a wide distribution of fissioning nuclei what becomes difficult the calculation process itself.

The systematization of cross-sections for symmetric and asymmetric fission in a wide range of nuclei, carried out in [33] showed that it is possible to use an empirical expression for estimating the probability of the different fission modes. In order to characterize this factor quantitatively, the authors introduced a critical value of the fissility parameter, in the form:

$$(Z^2/A)_{cr.} = 35.5 + 0.4(Z_f - 90). \tag{6}$$

According to [33], for the nuclei with Z^2/A values greater than the critical value, the symmetric fission mode was dominant, but, at smaller values of the fissility parameter, the main fission channel leads to asymmetric fragments.

The $(Z^2/A)_{cr.}$ for ^{241}Am, ^{238}U and ^{237}Np are equal to 37.5, 36.3, and 36.7, respectively. The mean masses of these fissioning nuclei at given proton energy were obtained in measurements $A \sim 227$, $Z \sim 95$ ($Z^2/A \sim 39.7$ for ^{241}Am); $A \sim 227$, $Z \sim 92$ ($Z^2/A \sim 37.29$ for ^{238}U); $A \sim 223.4$, $Z \sim 93$ ($Z^2/A \sim 38.72$ for ^{237}Np), so the symmetric fission component should increase. It is necessary to notice that the difference between Z^2/A and $(Z^2/A)_{cr.}$ is more for Am and Np nuclei, therefore symmetric fission in these nuclides is expressed more strongly. However, the possibility of the asymmetric fission for all fissioning nuclei remains at intermediate energy also because of broad mass and excitation energy distributions.

The energy of the highly excited system is removed by the evaporation of light particles prior to scission. From the Table 1 we can see that the mean masses of the fissioning nuclei $(\mathrm{A}_f)_{cal}$ are different from the target nuclei. The onset of the reaction is characterized by pre-equilibrium emission. It is followed by a cascade of neutrons evaporated from an equilibrated composite system. Both categories are referred to as pre-scission neutrons. When the system approaches the scission point, a new generation of neutrons is contributed from the nascent, accelerating or fully accelerated fragments. The multiplicity of these post-scission neutrons is a measure of the excitation energy remaining in the fragments. With increasing primary excitation energy of compound nucleus pre-scission and post-scission multiplicities increase with comparable rates.

The CRISP model calculations is capable of reproducing the number of neutrons observed for the fission reaction. The mass distributions, calculated for the compound nuclei after the cascade stage by the CRISP code, which considers competing deexcitation by sequential neutrons, γ-rays emission and by fission, are shown on Figure 4 (a, b, c). Figure 5 (a, b, c) shows the mass distributions of the fissioning nuclei at equilibrium stage in the reaction. Due to calculations of the above mentioned distributions, the neutron spectra were extracted and unfolded into pre-scission and post-scission contributions. The results are compared to the experimental data regarding emitted neutrons.

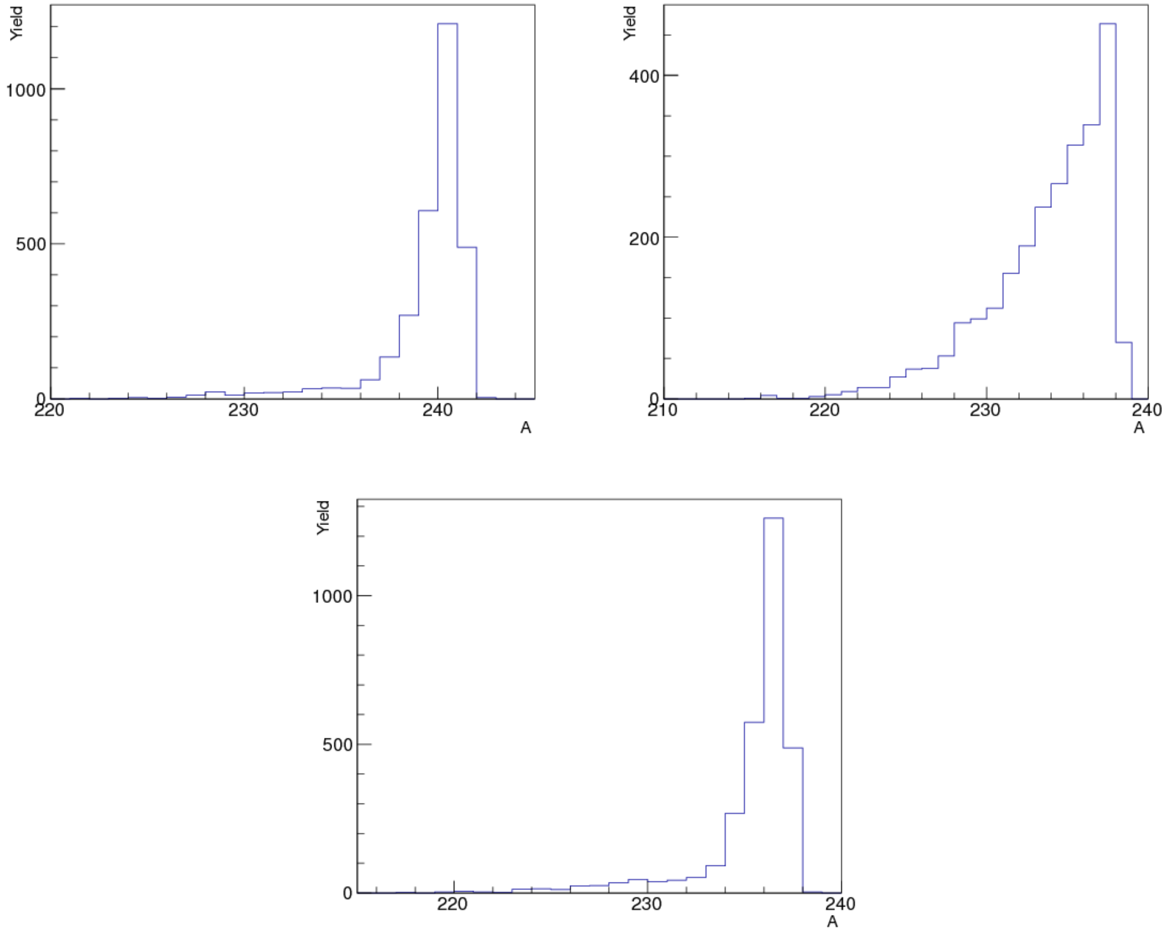

FIG. 4: Mass distributions of the compound nuclei after cascade stage of calculation for ^{241}Am (a), ^{238}U (b) and ^{237}Np (c) at proton energy 660 MeV.

The average pre-scission neutron multiplicity calculated correspond to 4.3, 6.5, and 3.3 for ^{241}Am, ^{238}U and ^{237}Np, respectively. The respective post-scission contribution correspond to 11.7, 4.5, and 11.7. The calculations reflect the total neutron multiplicity, which was experimentally found, quite well for all fissioning nuclei. Respectively 15, 12 and 14.6 neutrons were evaporated from ^{241}Am, ^{238}U and ^{237}Np targets.

Calculation by CRISP code made it possible to estimate the fissility for proton-induced fission and compare it with experimental. According to the well-known concept, the fissility is determined as the ratio of the fission cross-section (σ_{tot}) and the total cross section for inelastic interaction on a given nucleus (σ_{in}).

The dependence of fissility for ^{241}Am, ^{238}U and ^{237}Np targets from [1, 2] together with data for photon-induced fission of ^{238}U and ^{232}Th nuclei from [35, 36] and calculations data by CRISP code on parameter Z^2/A is shown on Fig. 6. The fission probabilities are in quantitative agreement with the experiments.

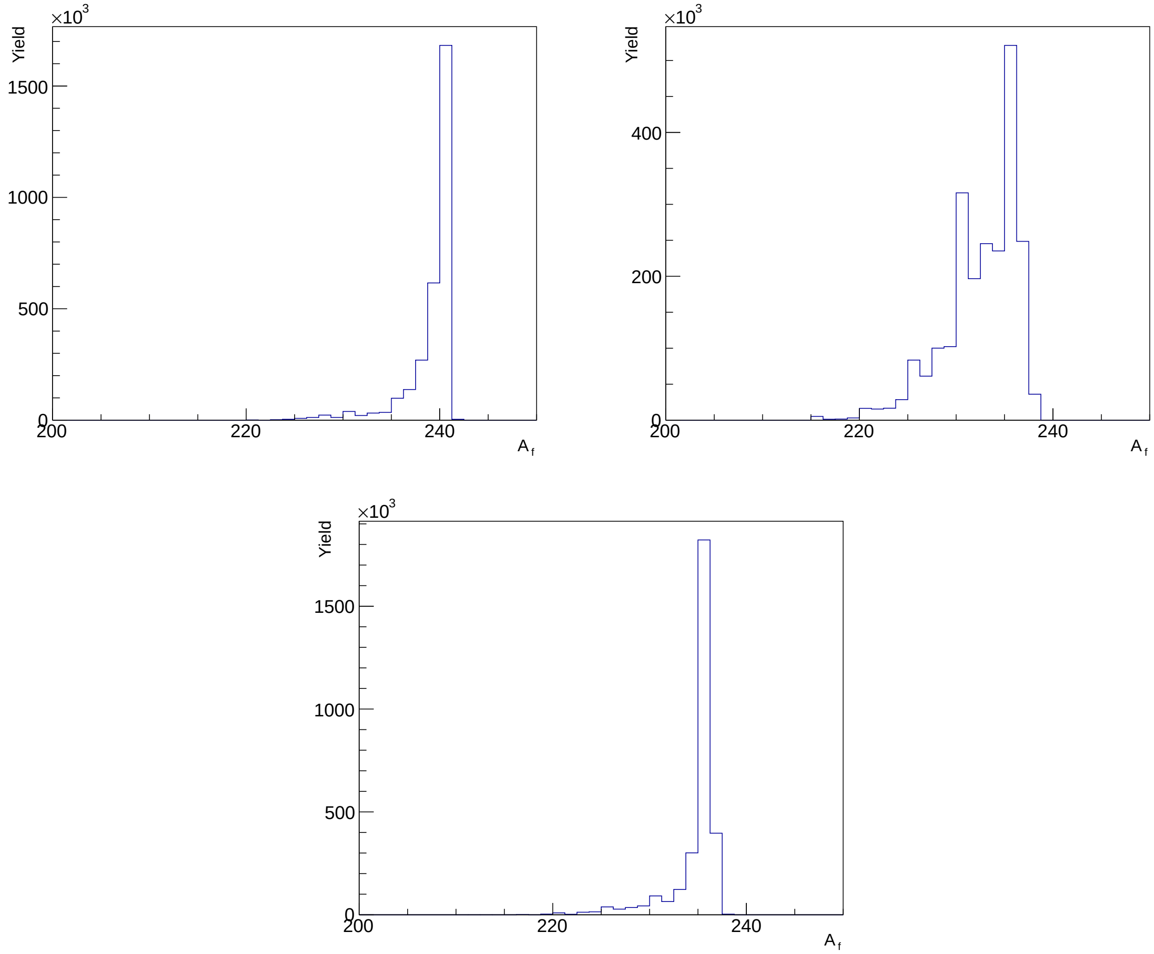

FIG. 5: Mass distributions of the fissioning nuclei at for ^{241}Am (a), ^{238}U (b) and ^{237}Np (c) at proton energy 660 MeV.

In [37], Fukahori *et al.* systematized data on the fission of actinide and lighter nuclei that was induced by protons, neutrons, and photons in the region of excitation energies from several tens of MeV units to 10 GeV. As a supplement to their systematics, they used data computed according to the FISCAL code. The objective of their study was to create a universal database for employing it in applied problems associated with the transmutation of fission fragments in subcritical systems. On the basis of systematizing experimental data and employing computed values in [37] was proposed an empirical formula for estimating fissilities of nuclei that is independent of the sort of interacting particles. The estimates obtained in the present study for the fissilities are in satisfactory agreement to experimental and computed data on reactions induced by protons, neutrons, and monoenergetic photons. A comparison of fissilities obtained in reactions induced by particles of different species makes it possible to exclude special features of primary interaction and to single out general regularities of the fission process.

The fissility of heavy nuclei at excitation energies above 40 MeV reaches a plateau, remaining below unity. This fact can be explained by the contribution of competing processes, such as the evaporation of neutrons, protons, and heavier particles at the preequilibrium stage of the interaction.

V. CONCLUSION

The modified CRISP model calculations, which takes into account different channel of fission was used to reproduced different aspects of proton-induced fission on ^{241}Am, ^{238}U and ^{237}Np targets at energy 660 MeV. Those calculations allowed direct evaluation of the spectrum of the compound and fissioning nuclei. The comparison with the calculated data was shown that the model describe correctly the main characteristics of charge distribution, such as the most probable charge for a given fission product mass chain and the width parameter. The mass yield of proton-induced

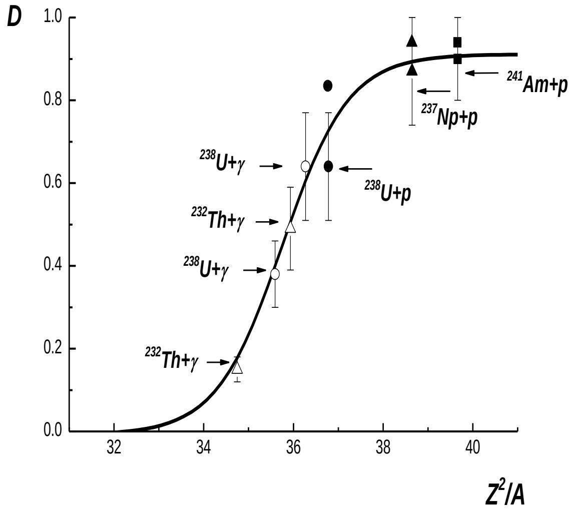

FIG. 6: Z^2/A dependence of fissility D. Presented symbols for experimental data are: p+241Am (■) [1, 2], p+238U (●) [1, 2], p+237Np (▲) [1, 2], γ+238U (○) [35, 36], γ+^{232}Th (△) [35, 36]. Calculations by CRISP are symbols without errors: p+241Am ■, p+238U (●), p+237Np (▲). The solid line is displayed as a guide.

fission fragments has been analyzed via multimodal fission approach. The results presented in this paper shows a fair agreement between calculation and experiment. The code reproduces totally the shape of the distribution. This fact shows that the model correctly takes into account the contribution of the symmetric and asymmetric modes. However, the code underestimates the absolute values of total fission cross-section for all targets under investigation. The neutron spectra of calculations were unfolded into prescission and postscission contributions. A determination of basic properties of individual components of the mass distribution has made it possible to estimate the absolute fissilities of ^{241}Am, ^{238}U and ^{237}Np nuclei and compare it with those from experiments. It was found out that the fissility value depends only slightly on the sort of incident particles. Thus, the mechanism of fission is determined by the properties of an excited fissile nucleus and is universal with respect to the nature of interacting particles.

Acknowledgment

G. Karapetyan is grateful to Fundação de Amparo à Pesquisa do Estado de São Paulo (FAPESP) 2011/00314-0. and to International Centre for Theoretical Physics (ICTP) under the Associate Grant Scheme.

---

[1] G. S. Karapetyan, A. R. Balabekyan, N. A. Demekhina, and J. Adam, Phys. At. Nucl. **72**, 911 (2009).

[2] A. R. Balabekyan, G. S. Karapetyan, N. A. Demekhina, *et al.*, Phys. At. Nucl. **73**, 1814 (2010).

[3] A. Deppman, S. B. Duarte, G. Silva, *et al.*, J. Phys. G: Nucl. Part. Phys. **30** 1991 (2004).

[4] T. Kodama, S. B. Duarte, K. C. Chung, *et al.*, Phys. Rev. Lett. **49**, 536 (1982).

[5] M. Goncalves, S. dePina, D. A. Lima, *et al.*, Phys. Lett. B **406**, 1 (1997).

[6] A. Deppman, O. A. P. Tavares, S. B. Duarte, *et al.*, Phys. Rev. Lett. **87**, 1 (2001).

[7] S. de Pina, *et al.*, Phys. Lett. B **434**, 1 (1998).

[8] A. Deppman, O. A. P. Tavares, S. B. Duarte, *et al.*, Comp. Phys. Comm **145**, 385 (2002).

[9] A. Deppman, O. A. P. Tavares, S. B. Duarte, *et al.*, Phys. Rev. C **66**, 067601 (2002).

[10] A. Deppman, G. Silva, S. Anefalos, *et al.*, Phys. Rev. C **73**, 1 (2006).

[11] E. Andrade-II, E. Freitas, O. A. P. Tavares, *et al.*, *Proc. Conf. on XXXI Worshop on Nuclear Physics in Brazil* **1139**, 64 (2009).

[12] S. A. Pereira, *et al.*, Nuc. Sci. and Eng. **159**, 102 (2008).

[13] S. Anefalos, A. Deppman, G. Silva, *et al.*, 2005 Braz. J. Phys. **35**, 912 (2005).

[14] S. Anefalos, A. Deppman, J. D. T. Arruda-Neto, *et al.*, *Proceedings of Int. Conf. on Nuclear Data for Science and Technology* **769**, 1299 (2004).

[15] S. T. Mongelli, J. R. Maiorino, S. Anefalos, *et al.*, Braz. J. Phys. **35**, 894 (2005).

[16] V. V. Pashkevich, Nucl. Phys. A **169**, 275 (1971).

[17] B. D. Wilkins, E. P. Steinberg, and R. R. Chasman, Phys. Rev. C **14**, 1832 (1976).

[18] U.Brosa, S. Grossman, and A. Muller, Z. Naturforschung **41a**, 1341 (1986).

[19] W.Younes, J.A.Becker, L.A.Bernstein, *et al.*, *CP610, Proceedings of Int. Nucl. Conf., INPC (2001).*

[20] H. Kudo, M. Maruyama, M. Tanikawa, *et al.*, Phys. Rev. C **57**, 178 (1998).

[21] M. C. Duijvestijn, A.J. Koning, *et al.*, Phys. Rev. C **59**, 776 (1999).

[22] C. Wagemans, P. Schillebeeckx and A. Deruytter, Nucl. Phys. A **502**, 287 (1989).

[23] Th. Weber, *et al.*, Nucl. Phys. A **502**, 279 (1989).

[24] J. L. Sida, *et al.*, Nucl. Phys. A **502**, 233 (1989).

[25] C. Bockstiegel , S. Steinhauser, K.-H. Schimdt, *et al.*, Nucl. Phys. A **802**, 12 (2008).

[26] F. J. Hambsch, *et al.*, Nucl. Phys. A **709**, 85 (2002).

[27] F. J. Hambsch, *et al.*, Nucl. Phys. A **726**, 248 (2003).

[28] H. Weigmann, H. H. Knitter and F. J. Hambsch, Nucl. Phys. A **502**, 177 (1989).

[29] T. Ohtsuki, *et al.*, Phys. Rev. C **40**, 2144 (1989).

[30] V. M. Maslov, Nucl. Phys. A **717**, 3 (2003).

[31] M. G. Itkis, *et al.*, Z. Phys. A **320**, 433 (1985).

[32] I. V. Pokrovsky, *et al.*, Phys. Rev. C **62**, 1 (2000).

[33] C. Chung and J.Hogan, Phys. Rev. C **25**, 899 (1982).

[34] V. A. Rubchenya, Phys. Rev. C **75**, 054601 (2007).

[35] N. A. Demekhina and G. S. Karapetyan, Phys. At. Nucl. **71**, 27 (2008).

[36] N. A. Demekhina and G. S. Karapetyan, Phys. At. Nucl. **73**, 24 (2010).

[37] T. Fukahori, O. Iwamoto, and S. Chiba, *Proc. of the 7th Intern. Conf. on Nucl. Criticality Safety, Japan*, 144 (2003).